J. Mol. Microbiol. Biotechnol. (2001) 3(3): 347-354.

Three-Dimensional Structures of Protein-Protein Complexes in the *E. coli* PTS

Alan Peterkofsky[1]*, Guangshun Wang[2], Daniel S. Garrett[2], Byeong Ryong Lee[1], Yeong-Jae Seok[3], and G. Marius Clore[2]*

[1]Laboratory of Biochemical Genetics, National Heart, Lung and Blood Institute, National Institutes of Health, Bldg. 36, Rm. 4C-11, Bethesda, MD 20892-4036, USA
[2]Laboratory of Chemical Physics, National Institute of Diabetes and Digestive and Kidney Diseases, Bldg. 5, Rm. B1-30I, Bethesda, MD 20892, USA
[3]School of Biological Sciences, Seoul National University, Seoul 151-742, Korea

Abstract

The bacterial phosphoenolpyruvate:sugar phosphotransferase system (PTS) includes a collection of proteins that accomplish phosphoryl transfer from phosphoenolpyruvate (PEP) to a sugar in the course of transport. The soluble proteins of the glucose transport pathway also function as regulators of diverse systems. The mechanism of interaction of the phosphoryl carrier proteins with each other as well as with their regulation targets has been amenable to study by nuclear magnetic resonance (NMR) spectroscopy. The three-dimensional solution structures of the complexes between the N-terminal domain of enzyme I and HPr and between HPr and enzyme IIA^{Glc} have been elucidated. An analysis of the binding interfaces of HPr with enzyme I, IIA^{Glc} and glycogen phosphorylase revealed that a common surface on HPr is involved in all these interactions. Similarly, a common surface on IIA^{Glc} interacts with HPr, IIB^{Glc} and glycerol kinase. Thus, there is a common motif for the protein-protein interactions characteristic of the PTS.

Introduction

A number of constitutive and inducible sugar transport systems of *E. coli* are characterized by the presence in the cytoplasmic membrane of specific sugar-recognition proteins (permeases) that can effect the process of sugar transport coupled to sugar phosphorylation (Postma *et al.*, 1996). The source of the phosphoryl group is intracellular phosphoenolpyruvate (PEP). From an energetic standpoint, it would be possible for PEP to directly phosphorylate the cytoplasmic component of the permease. However, the process is more complicated; there are a number of cytoplasmic proteins that mediate phosphoryl transfer from PEP to the permeases (enzymes II). Enzyme I (EI) is directly autophosphorylated by PEP and P-enzyme I effects phosphoryl transfer to enzymes II via the phosphoryl carrier protein, HPr. The complexity of this system (the phosphoenolpyruvate:sugar phosphotransferase system, PTS) is apparently due to the multi-functional capacity of the PTS to regulate other systems in addition to catalyzing sugar transport (see Figure 1). Thus, enzyme I may regulate the Krebs cycle via phosphorylation of acetate kinase (Fox *et al.*, 1986). HPr has been shown to regulate the activity of glycogen phosphorylase (Seok *et al.*, 1997). The enzyme I-HPr pair appears to play a role in the regulation of chemotaxis (Lux *et al.*, 1995). The enzyme II specific for glucose (IIA^{Glc}) is capable of multiple regulatory interactions. Depending on its state of phosphorylation, it influences the activity of adenylate cyclase, glycerol kinase and non-PTS permeases (Postma *et al.*, 1996).

An understanding of the mechanisms involved in the process of phosphoryl transfer via the PTS, as well as the participation of the PTS proteins in regulatory processes, is greatly assisted by visualization of the three-dimensional structures of the interacting species of the protein components. The individual proteins of the PTS (enzyme I, HPr, IIA) have been extensively characterized by x-ray crystallography and NMR. However, with the exception of the glycerol kinase-IIA^{Glc} complex (Feese *et al.*, 1994), none of the complexes of PTS proteins with each other or with regulatory partners has been successfully crystallized.

Nuclear magnetic resonance (NMR) spectroscopy has been used successfully by us to bypass the problems associated with crystallization of protein-protein complexes. The three-dimensional solution structures of the complexes between the aminoterminal domain of enzyme I and HPr as well as that between HPr and IIA^{Glc} have been solved. The characteristics of these PTS protein complexes are described in this review.

The Enzyme I-HPr Complex

The first step of the PTS involves an autophosphorylation by PEP of enzyme I. The binding site for PEP is located in the C-terminal domain of a two-domain structure, while the active site (His189) for phosphorylation is in the N-terminal domain (LiCalsi *et al.*, 1991). Phospho-EI transfers its phosphoryl group to the active site His15 of HPr. While the aminoterminal half of EI (EIN) is incapable of autophosphorylation by PEP, this protein domain retains the capacity to reversibly transfer a phosphoryl group to HPr, indicative that the binding site for HPr resides in EIN (Seok *et al.*, 1996). Attempts to deduce the crystallographic structure of intact EI have thus far been unsuccessful, but the structure of EIN has been solved by both x-ray crystallography (Liao *et al.*, 1996) and NMR (Garrett *et al.*, 1997a). Mixtures of EI or EIN with HPr were subjected to trials for co-crystallization with no success.

*For correspondence. Email alan@codon.nih.gov or clore@speck.niddk.nih.gov.

The EIN-HPr complex (~40 kDa) is one of the largest structures solved by NMR (Garrett *et al.*, 1999). The structure determination made use of multidimensional heteronuclear NMR spectroscopy using multiple combinations of isotopically labeled (^{15}N, ^{13}C and/or ^{2}H) proteins to simplify the spectra for assignment purposes and to observe specifically intermolecular nuclear Overhauser enhancement (NOE) contacts between EIN and HPr. In addition, residual dipolar couplings were employed to provide long-range orientational information which is highly valuable for determining the orientation of the two proteins in the complex.

Two views illustrating the overall complex are shown as ribbon diagrams in Figure 2. EIN comprises two subdomains: the α domain (residues 33-143), shown in red, is a four helix bundle comprising helices H1, H2/H2', H3 and H4; the α/β domain (residues 1-20 and 148-230), shown in blue, comprises a β-sandwich, formed by a four-stranded parallel β-sheet (β1-β4) and a three-stranded antiparallel β-sheet (β1, β5, β6), as well as three short helices (H5-H7); in addition, there is a long C-terminal helix (H8) that serves as a linker to the C-terminal domain of EI. HPr comprises three helices and a four stranded antiparallel β-sheet. The structures of EIN and HPr in the complex are very similar to those in the free state. The interaction of EIN with HPr involves exclusively the α-subdomain of EIN, consistent with previous chemical shift perturbation mapping (Garrett *et al.*, 1997b).

A detailed summary of the contacts between the two proteins is shown in Figure 3. There are 44 residues at the interface, 21 from EIN and 23 from HPr. The majority of the contacts between the two proteins are hydrophobic in nature. Hydrophobic residues involved in three or more intermolecular contacts are: Ala71, Ile72, Met 78, Leu79, Leu115, Tyr122, Leu123 and Arg126 of EIN and Thr16, Arg17, Ala20, Leu 47, Phe48 and Thr52 of HPr. In addition, there are 11 intermolecular electrostatic interactions, including two side chain to backbone hydrogen bonds and six salt bridges. The hydroxyl group of Tyr122 and the guanidinium group of Arg126 of EIN are hydrogen-bonded to the backbone carbonyl of Leu14 of HPr. The salt bridges comprise the following pairs of EIN and HPr residues, respectively: Glu67 and Arg17, Glu68 and Arg17, Glu74 and Lys24, Asp82 and Lys27, Glu84 and Lys45 and Glu84 and Lys49. In addition, the carboxylate of Asp82 is not only involved in an intermolecular salt bridge but also accepts two hydrogen bonds from the backbone amides of Glu84 and Leu85 which serve to stabilize the kink between helices 2 and 2' of EIN. Finally, there are three side chain-side chain hydrogen bonding interactions between Asp129 and Thr16, Glu84 and Ser46 and Arg126 and Gln51.

Significant aspects of the transition state between EIN and HPr are shown in Figure 4. EIN and HPr are phosphorylated at the Nε2 atom of His 189 and the Nδ1 atom of His15, respectively. In the unphosphorylated form of the complex, His189 makes no contacts with HPr and the Nε2 atom of His189 accepts a hydrogen bond from the hydroxyl proton of Thr168, just as it does in free EIN, so that it is directed away from the Nδ1 atom of His15. Modeling of the transition state was accomplished by adding a phosphoryl group (with the appropriate trigonal bipyramidal geometry) to the coordinates halfway between His189 of EIN and His15 of HPr, removing the intramolecular NOE between the side chain of His189 and the methyl group of Thr168 and repeating the simulated annealing calculations on the basis of the remaining experimental NMR restraints. This led to the structure shown in Figure 4 in which the only significant structural change involved a flipping of the side chain χ_2 angle of His189 by about 150^o, permitting the Nε2 atom of His189 to come into close proximity to the Nδ1 atom of His15.

The pentacoordinate phosphorous in the transition state is located at the bottom of a cleft formed by the N-terminal end of helix 2 of EIN, helix 6 of EIN and the N-terminal end of helix 1 of HPr. From a structural standpoint, the transition state is stabilized in favor of phosphorylated HPr relative to phosphorylated EIN. In addition, phosphorylation of EIN destabilizes EIN, in part due to the loss of the hydrogen bond between His189 and Thr168, which also favors phosphoryl transfer from EIN to HPr. Both factors contribute to stimulating phosphotransfer in the PTS in the appropriate direction.

The HPr-IIA^{Glc} Complex

Phosphorylated HPr is a general phosphoryl donor to all PTS enzymes II (see Figure 1). That phosphotransfer activity accomplishes the transition from the early general phosphotransfer portion of the PTS cascade to the sugar-specific arms of the pathway. Of particular interest is the IIA of the glucose-specific transporter (IIA^{Glc}). This protein functions not only as an intermediate in glucose transport but also as a regulator of non-PTS permeases as well as adenylate cyclase (Figure 1).

Three-dimensional structures of *E. coli* HPr and IIA^{Glc} have been elucidated by x-ray crystallography and NMR (Herzberg and Klevit, 1994). Consequently, the solution of the structure of the *E. coli* HPr-IIA^{Glc} complex by NMR was undertaken and successfully completed (Wang *et al.*, 2000a).

As with the previously discussed EIN-HPr structure, the solution structure of the HPr-IIA^{Glc} complex was solved by multidimensional heteronuclear NMR spectroscopy using a combination of isotopically labeled proteins. In the case of the HPr-IIA^{Glc} complex, the structure calculation took advantage of a novel procedure that makes use of rigid body minimization to dock the structures followed by constrained/restrained simulated annealing to refine the interfacial side chain position (Clore, 2000). This was possible because no significant backbone conformational changes occur as a result of complex formation.

The HPr-IIA^{Glc} complex, respresented as a ribbon diagram, is shown in Figure 5. As previously determined, HPr is represented as an open-faced α/β sandwich protein with three α-helices sitting on top of the four-stranded antiparallel β-sheet. The IIA^{Glc} structure is composed of mainly β-strands in a sandwich with six antiparallel strands on each side. The inter-protein binding surface involves a complementary fit of a convex region on HPr (helices 1 and 2) and a concave region on IIA^{Glc} (β-strands 5, 6, 7 and 10). The 41 residues at the interface include 18 from HPr and 23 from IIA^{Glc}.

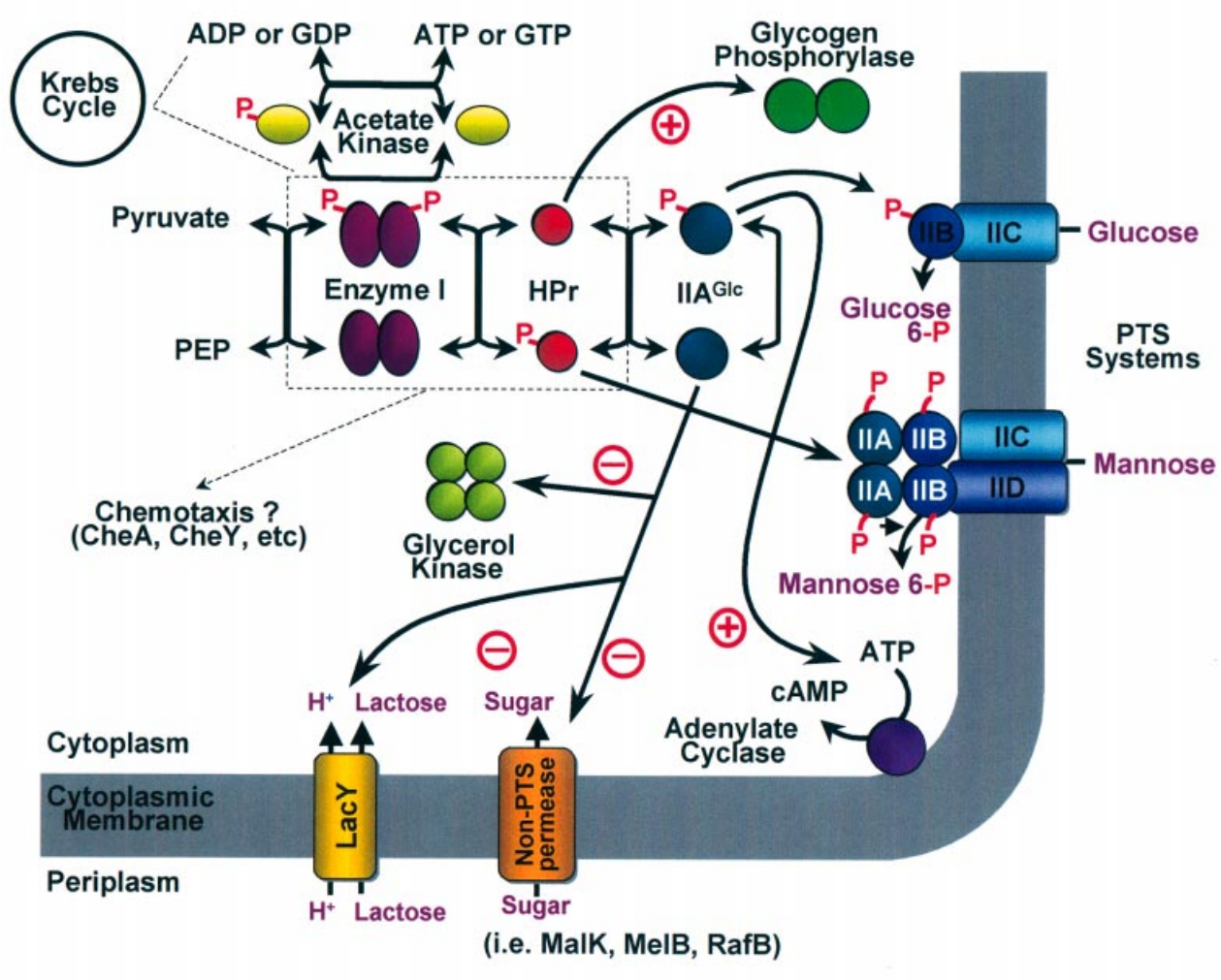

Figure 1. The PTS and components with which it interacts.

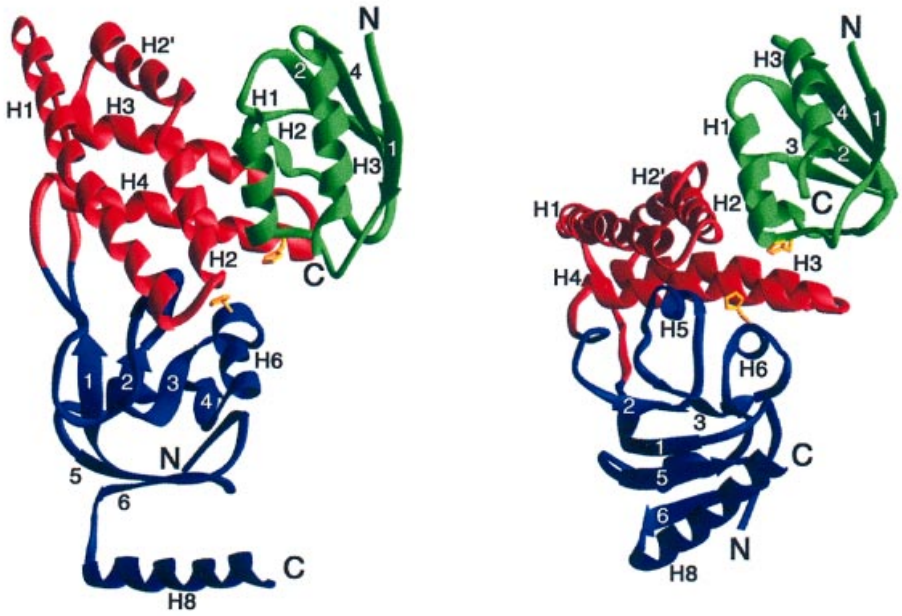

Figure 2. Structure of the EIN-HPr complex. Ribbon diagrams showing two views of the complex. HPr, green; α-domain of EIN, red; α/β-domain and C-terminal helix of EIN, blue; side chains of His189 of EIN and His15 of HPr, gold (from Garrett *et al.*, 1999).

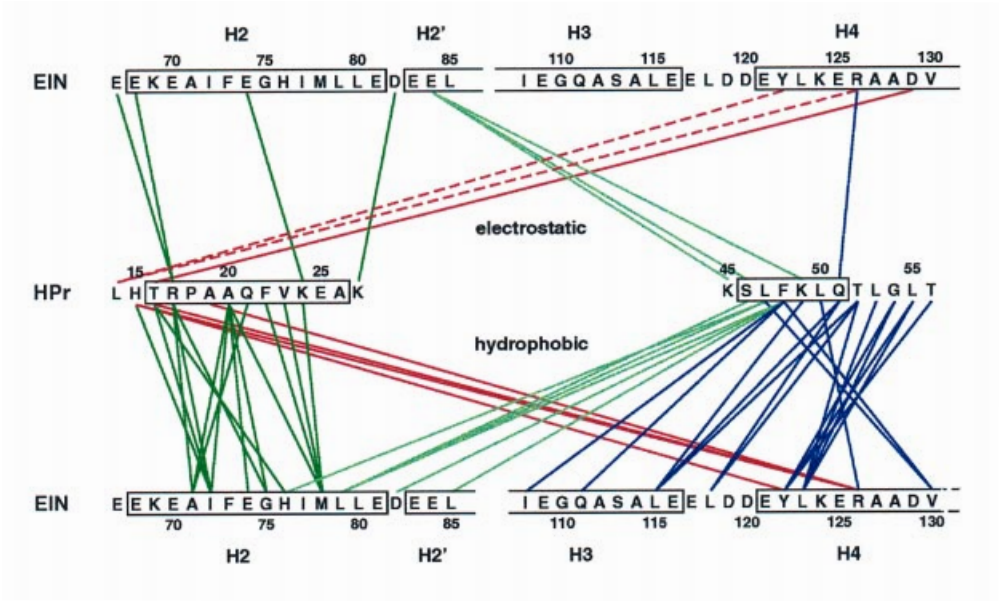

Figure 3. EIN-HPr interactions. Summary of electrostatic (top) and van der Waals (bottom) interactions between EIN and HPr. Red lines indicate interactions between helix 1 of HPr and helix 4 of EIN, green lines the interactions between helices 1 and 2 of HPr and helices 2 and 2' of EIN, and the blue lines between helix 2 of HPr and helices 3 and 4 of EIN. The dashed lines for the electrostatic interactions show the side chain-backbone hydrogen bonds (from Garrett *et al.*, 1999).

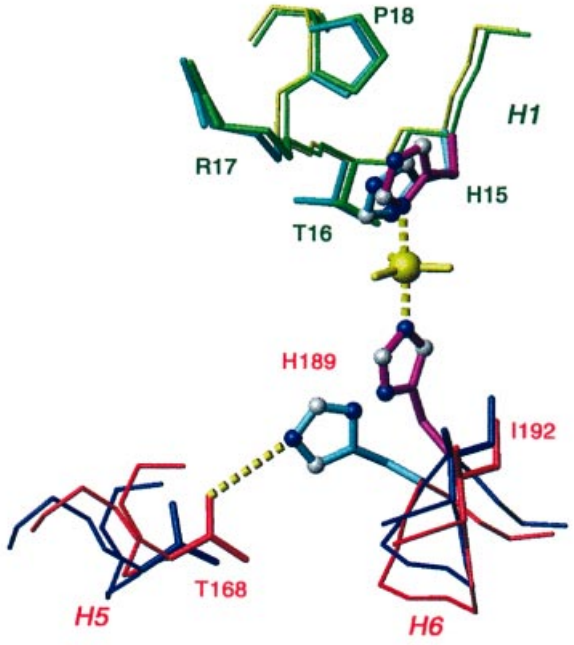

Figure 4. The transition state of the EIN-HPr complex. Helices 5 and 6 of EIN and helix 1 of HPr in the unphosphorylated complex is superimposed on the transition state. The change in conformation of His189 of EIN and His15 of HPr, as well as the lateral displacement of helices 5 and 6 of EIN is shown (from Garrett *et al.*, 1999).

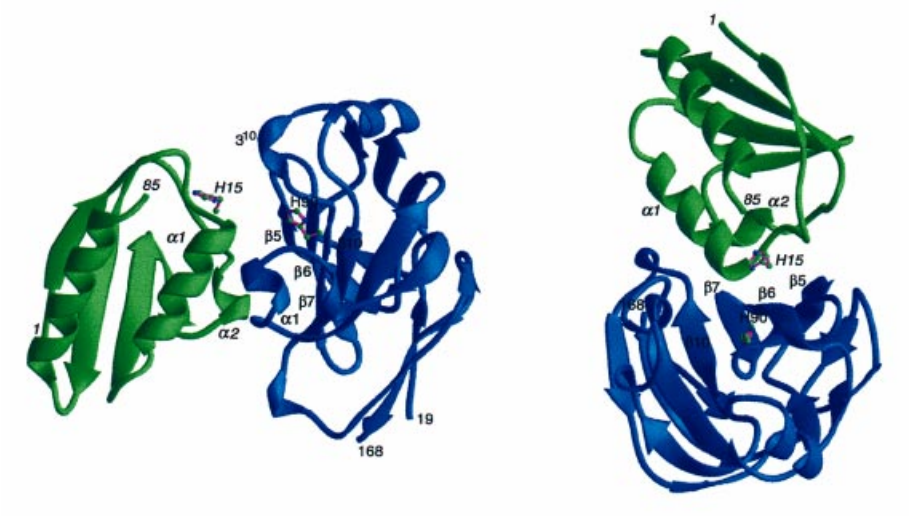

Figure 5. Ribbon diagrams of the HPr-IIA^{Glc} complex. Two views are shown; HPr, green; IIA^{Glc}, blue. The location of the active site histidines (His15 of HPr and His90 of IIA^{Glc}), as well as the secondary structure elements in the vicinity of the interface, are shown (from Wang *et al.*, 2000a).

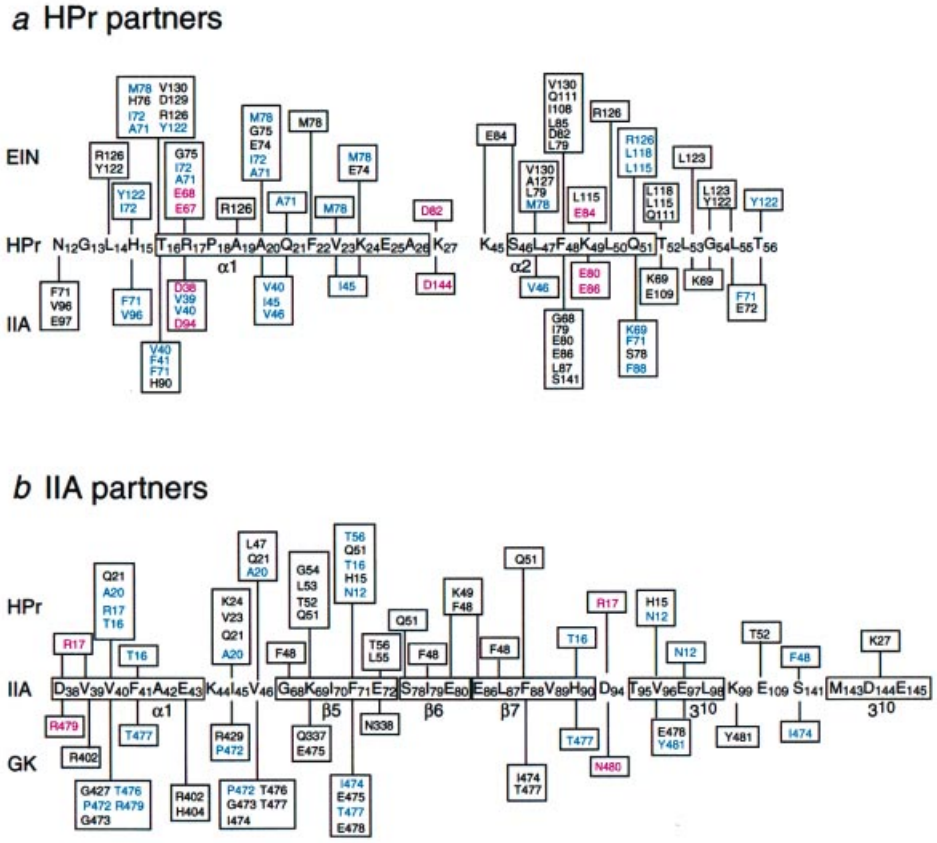

Figure 6. Interactions between partner proteins. (A) the interactions between HPr and its partners EIN and IIA^{Glc} (denoted IIA); (B) the interactions between IIA^{Glc} and its partners HPr and glycerol kinase (denoted GK). Hydrophobic interactions, blue; electrostatic interactions, red (from Wang *et al.*, 2000a).

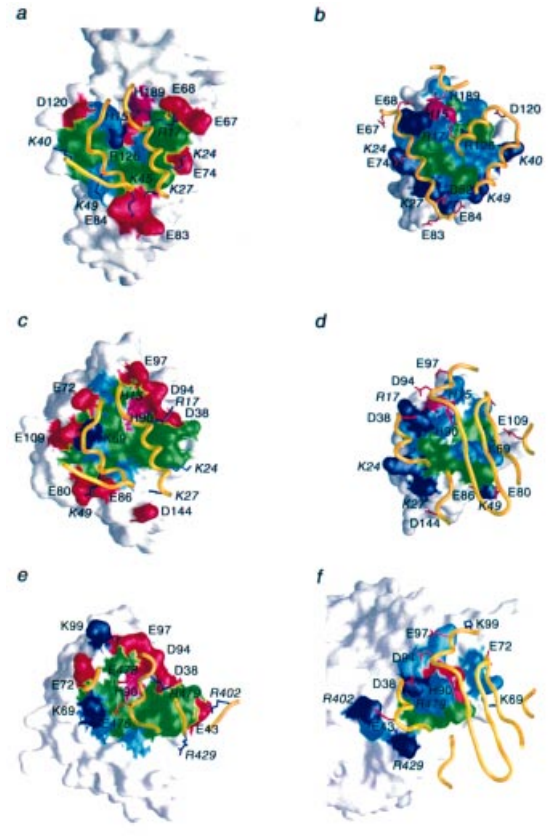

Figure 7. Surface representations illustrating the binding surfaces involved in the (A and B) EIN-HPr, (C and D) HPr-IIA^{Glc} and (E and F) IIA^{Glc}-GK complexes. The HPr binding surfaces on EIN and IIA^{Glc} are shown in (A) and (C), respectively; the EIN and IIA^{Glc} binding surfaces on HPr are shown in (B) and (D), respectively; the GK binding surface on IIA^{Glc} is shown in (E); the IIA^{Glc} binding surface on GK is shown in (F). The binding surfaces are color coded with hydrophobic residues in green, polar residues in light blue, the active site histidines in purple, positively charged residues in dark blue and negatively charged residues in red. The relevant portion of the backbone of the partner protein is shown as a gold ribbon with positively charged side chains in dark blue and negatively charged ones in red. Only charged residues and the active site histidines are labeled, with residues from HPr and GK denoted in italic. Note that although the active site histidines of EIN (His189) and IIA^{Glc} (His90) are in close contact with His15 of HPr, their direction of approach is different: His189 (EIN) approaches His15 from above (B), while His90 (IIA^{Glc}) approaches His15 from below (D) (from Wang *et al.,* 2000a).

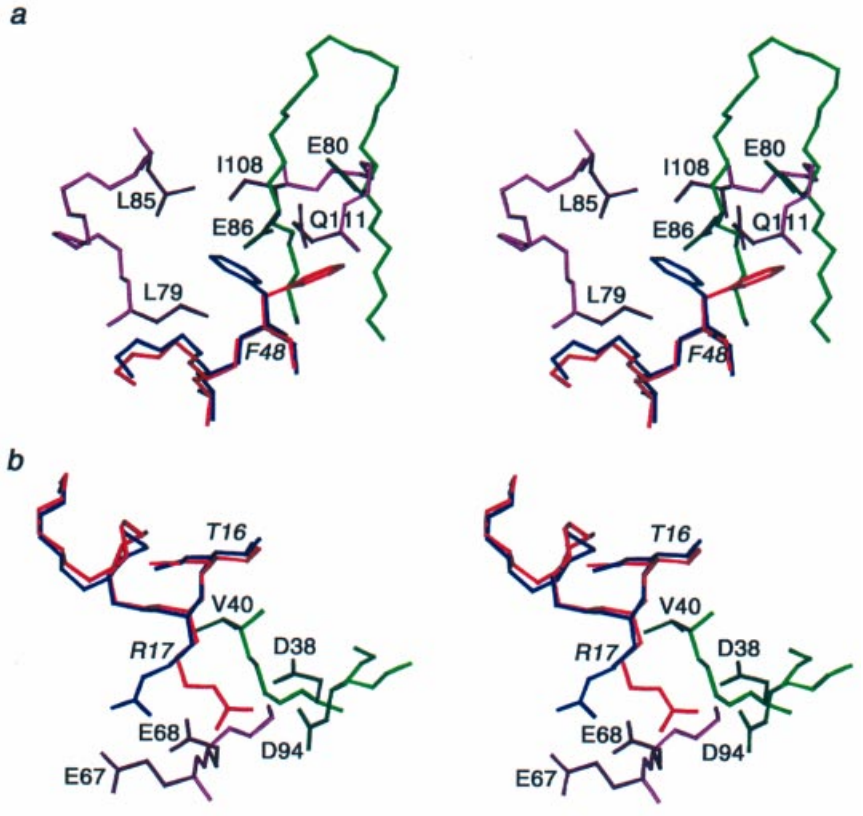

Figure 8. HPr side chain plasticity. (A) stereoview of superposition of selected regions of the interfaces of the HPr-IIA^{Glc} and EIN-HPr complexes showing the different conformations of Phe48 of HPr; (B) superposition of regions of the two complexes showing the different conformations of Arg17 of HPr. HPr in the HPr-IIA^{Glc} complex, red; HPr in the EIN-HPr complex, blue; EIN, purple; IIA^{Glc}, green (from Wang *et al.*, 2000a).

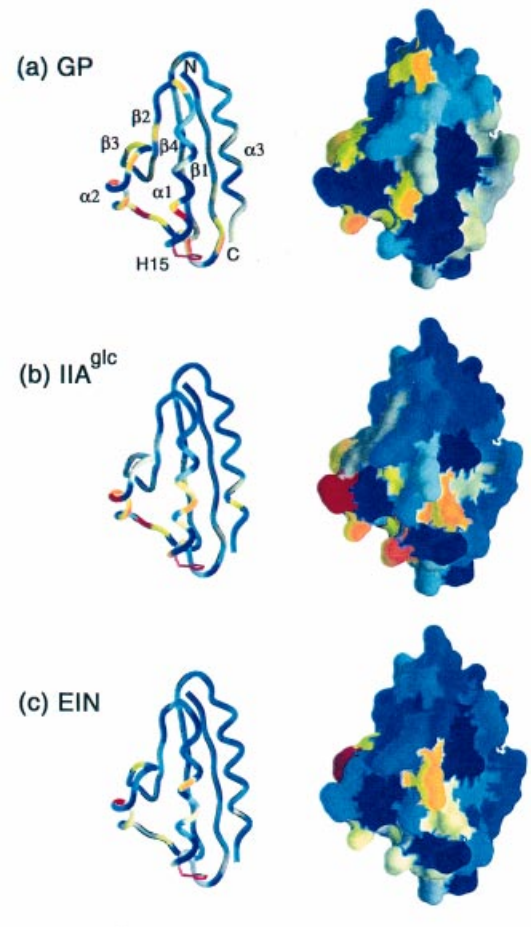

Figure 9 . Binding surface on HPr for its partners. (a) the binding surface for glycogen phosphorylase (GP); (b) the binding surface for IIA^{Glc}; (c) the binding surface for EIN. Backbone chemical shift perturbations were mapped onto a ribbon diagram of HPr (left side of figure) and the accessible surface of HPr (right side of figure). The magnitude of the shifts are shown in colors varying from blue (no shift) through yellow (intermediate shift) to red (maximum shift). Secondary structure elements are labeled in the ribbon diagram shown in (a). The side chain of His15 of HPr is shown in red on the ribbon diagram (from Wang *et al*., 2000b).

The contacts between HPr and IIA^{Glc} are shown in Figure 6. The central portion of each binding surface is predominantly hydrophobic, consisting in the case of HPr of the methyl groups of Thr16, Ala20, Val23 and Leu47 and the aromatic ring of Phe48, and in the case of IIA^{Glc} of a ring of three phenyalanine residues, 41, 71 and 88, interspersed by three valines, 40, 46 and 96. The central hydrophobic patch is surrounded in both cases by polar and charged residues. The latter are entirely positive in the case of HPr and negative for IIA^{Glc}.

It was possible to successfully model the transition state between HPr and IIA^{Glc} starting with the coordinates for the complex and introducing a phosphoryl group in the appropriate trigonal bipyramidal geometry halfway between the two active site histidines followed by rigid body minimization and constrained/restrained simulated annealing on the basis of the experimental NOE and dipolar coupling restraints. In the resultant model, the planes of the imidazole rings of His15 of HPr and His90 of IIA^{Glc} are oriented at ~90^o to each other. In the complex, the orientations of the imidazole ring of His15 and the side chain of Arg17 of HPr are stabilized by a number of hydrophobic and electrostatic contacts.

In the case of HPr (Figure 6A), a comparison is made to the contacts previously determined for the HPr-EIN surface. Similarly, in the case of IIA^{Glc} (Figure 6B), a comparison is made with the contacts involved in the surface with glycerol kinase (GK). The binding surfaces for EIN and IIA^{Glc} on HPr are very similar, sharing 17 residues in common, out of a total of 18 that interact with IIA^{Glc} and 23 with EIN (Figure 6A). The main feature of this common convex binding surface is a central hydrophobic core surrounded by a ring of polar and positively charged residues. The backbone scaffolds used for the HPr binding surface on EIN and IIA^{Glc} are entirely different. The HPr binding surface on EIN is composed of α-helices while that on IIA^{Glc} is mainly β-sheet. However, surface representations of the two binding surfaces show them to be similar in both shape and residue distribution (see Figure 7). The binding surfaces of both EIN and IIA^{Glc} are concave and circular with a hydrophobic core surrounded by a ring of polar and negative charges that are complementary to the positively charged binding surface on HPr.

In order to achieve successful complexes with both EIN and IIA^{Glc}, side chain plasticity of residues on HPr is required, as shown in Figure 8. Phe48 is involved in some important hydrophobic contacts. In the EIN-HPr complex, the torsion angle of Phe48 is in a conformation that permits it to interact with Leu79, Leu85, Ile108 and Gln111 of EIN (Figure 8A). However, in the HPr-IIA^{Glc} complex, the side chain of Phe48 is in a different conformation, allowing it to interact with the backbone of β6 and 7 of IIA^{Glc}. Thus, Phe48 adopts specific conformations depending on its interacting partner.

The plasticity of Arg17 of HPr is shown in Figure 8B. In the EIN-HPr complex, the side chain is in a conformation that allows it to form ion pairs with the carboxylates of Glu67 and 68 of EIN. A different conformation of the Arg17 side chain is found in the HPr-IIA^{Glc} complex, allowing it to form ion pairs with the carboxylates of Asp38 and 94 of IIA^{Glc}.

As is the case with the multiple complexes involving HPr, the complex of IIA^{Glc} with multiple partners shows an overlap (Figure 6B). The surface on IIA^{Glc} that interacts with HPr has 23 residues, 16 of which also interact with GK. The scaffolds comprising the IIA^{Glc} binding surfaces on HPr and GK are also distinct. While the binding surface on HPr involves two helices, that on GK has one short helix and parts of three loops. The IIA^{Glc} binding surface presented to both HPr and GK is concave. Further, the location of the hydrophobic residues on IIA^{Glc} involved in both binding surfaces are approximately the same; this is also the case for the polar and positively charged residues.

The protein-protein complexes elucidated show that there is extensive overlap in the binding surface on HPr for the interaction with EI and IIA^{Glc} (Figure 6A), as well as on IIA^{Glc} for the interactions with HPr and GK (Figure 6B). This is consistent with the idea that the active site regions of HPr and IIA^{Glc} must be in contact with their interacting partners in order to achieve the appropriate phosphotransfer or regulation mechanisms.

Common Interface on HPr for Interaction with Partner Proteins

In the previous discussion, it has become apparent that the region of HPr that binds to either EI or IIA^{Glc} is similar. Further, the surface on IIA^{Glc} that binds to HPr is similar to that interacting with GK. The finding that HPr serves as an allosteric regulator of *E. coli* glycogen phosphorylase (Seok *et al.*, 1997) prompted a study to extend the proposition that a common face on HPr interacts with all of its partner proteins. Two dimensional ^1H-^{15}N heteronuclear correlation spectra of ^{15}N-HPr in the presence of unlabeled glycogen phosphorylase revealed chemical shift deviations that were similar to those previously observed for the interaction of HPr with EIN and IIA^{Glc} (Wang *et al.*, 2000b). A visualization of the nature of the interaction of HPr with the three proteins is shown in Figure 9. The chemical shift perturbations resulting from the interaction of HPr with (a) glycogen phosphorylase, (b) IIA^{Glc} and (c) EIN are mapped on a ribbon diagram of HPr (left side of the figure) and on an accessible surface representation (right side of figure). In all the cases, the residues most perturbed form a cluster in a near-identical region of the three-dimensional structure of HPr; a contiguous surface composed of helix 1, helix 2, the carboxyterminus of helix 3 and the loops between β-strand 1 and helix 1, β-strand 3 and helix 2, and helix 2 and β-strand 4. EIN and IIA^{Glc} perturb a somewhat narrower region on HPr than does glycogen phosphorylase. This is consistent with the finding of a 2-3 order of magnitude higher binding affinity for glycogen phosphorylase than for EIN and IIA^{Glc} (Seok *et al.*, 1997).

Concluding Remarks

NMR studies have made it possible to uncover the nature of the protein-protein interactions involving the proteins of the PTS (Garrett *et al.*, 1999;Wang *et al.*, 2000a). The elucidation of the three-dimensional solution structures has revealed that the partner-partner interaction involves a concave-convex surface complementarity, although the precise structures of different proteins that bind to HPr or IIA^{Glc} are dissimilar. For all the cases studied thus far, the binding interfaces on HPr or IIA^{Glc} for its partners show

extensive overlap. This pattern suggests that, in the PTS, it is necessary for one protein to be released from its partner before it can interact with the next component of the cascade and that there is not a functional multiprotein complex.

Acknowledgement

We thank Melissa Sondej for providing Figure 1.

References

Clore, G.M. 2000. Accurate and Rapid Docking of Protein-Protein Complexes on the Basis of Intermolecular Nuclear Overhauser Enhancement Data and Dipolar Couplings by Rigid Body Minimization. Proc.Natl.Acad.Sci., USA. 97: 9021-9025.

Feese, M., Pettigrew, D.W., Meadow, N.D., Roseman, S., and Remington, S.J. 1994. Cation-promoted association of a regulatory and target protein is controlled by protein phosphorylation. Proc.Natl.Acad.Sci., USA. 91: 3544-3548.

Fox, D.K., Meadow, N.D. and Roseman, S. 1986. Phosphate Transfer between Acetate Kinase and Enzyme I of the Bacterial Phosphotransferase System. J. Biol. Chem. 261: 13498-13503.

Garrett, D.S., Seok, Y.-J., Liao, D.-I., Peterkofsky, A., Gronenborn, A.M., and Clore, G.M. 1997a. Solution structure of the 30 kDa N-terminal domain of enzyme I of the *Escherichia coli* phosphoenolpyruvate:sugar phosphotransferase system by multidimensional NMR. Biochemistry 36: 2517-2530.

Garrett, D.S., Seok, Y.-J., Peterkofsky, A., Clore, G.M., and Gronenborn, A.M. 1997b. Identification by NMR of the Binding Surface for the Histidine-Containing Phosphocarrier Protein HPr on the N-Terminal Domain of Enzyme I of the *Escherichia coli* Phosphotransferase System. Biochemistry 36: 4393-4398.

Garrett, D.S., Seok, Y.-J., Peterkofsky, A., Gronenborn, A.M., and Clore, G.M. 1999. Solution structure of the 40,000 Mr phosphoryl transfer complex between the N-terminal domain of enzyme I and HPr. Nature Struct.Biol. 6: 166-173.

Herzberg, O., and Klevit, R. 1994. Unraveling a bacterial hexose transport pathway. Current Opinion in Structural Biology 4: 814-822.

Liao, D.-I., Silverton, E., Seok, Y.-J., Lee, B.R., Peterkofsky, A., and Davies, D.R. 1996. The first step in sugar transport: crystal structure of the amino terminal domain of enzyme I of the *E. coli* PEP:sugar phosphotransferase system and a model of the phosphotransfer complex with HPr. Structure 4: 861-872.

LiCalsi, C., Crocenzi, T.S., Freire, E., and Roseman, S. 1991. Sugar Transport by the Bacterial Phosphotransferase System. Structural and Thermodynamic Domains of Enzyme I of *Salmonella typhimurium*. J. Biol. Chem. 266: 19519-19527.

Lux, R., Jahreis, K., Bettenbrock, K., Parkinson, J.S., and Lengeler, J.W. 1995. Coupling the phosphotransferase system and the methyl-accepting chemotaxis protein-dependent chemotaxis signaling pathways of *Escherichia coli*. Proc. Natl. Acad. Sci. USA. 92: 11583-11587.

Postma, P.W., Lengeler, J.W., and Jacobson, G.R. 1996. Phosphoenolpyruvate:Carbohydrate Phosphotransferase Systems. In: *Escherichia coli* and *Salmonella:* Cellular and Molecular Biology, ed. F.C.Neidhardt. Washington, DC: ASM Press, 1149-1174.

Seok, Y.-J., Lee, B.R., Zhu, P.-P., and Peterkofsky, A. 1996. Importance of the carboxy-terminal domain of enzyme I of the *Escherichia coli* phosphoenolpyruvate:sugar phosphotransferase system for phosphoryl donor specificity. Proc.Natl.Acad.Sci., USA 93: 347-351.

Seok, Y.-J., Sondej, M., Badawi, P., Lewis, M.S., Briggs, M.C., Jaffe, H., and Peterkofsky, A. 1997. High Affinity Binding and Allosteric Regulation of *E. coli* Glycogen Phosphorylase by the Histidine Phosphocarrier Protein, HPr. J. Biol. Chem. 272: 26511-26521.

Wang, G., Louis, J.M., Sondej, M., Seok, Y.-J., Peterkofsky, A., and Clore, G.M. 2000a. Solution structure of the phosphoryl transfer complex between the signal transducing proteins HPr and $IIA^{Glucose}$ of the *Escherichia coli* phosphoenolpyruvate:sugar phosphotransferase system. EMBO J 19; 5635-5649 .

Wang, G., Sondej, M., Garrett, D.S., Peterkofsky, A., and Clore,G.M. 2000b. A Common Interface on Histidine-containing Phosphocarrier Protein for Interaction with Its Partner Proteins. J. Biol. Chem. 275: 16401-16403.